

# Global spin alignment of $\phi$ and $K^{*0}$ vector mesons in Au+Au collisions from RHIC BES-II program

Gavin Wilks<sup>1,\*</sup>, for the STAR Collaboration

<sup>1</sup>The University of Illinois at Chicago, 1200 W Harrison St, Chicago, IL 60607

**Abstract.** Global spin alignment is a preferential alignment of a particle's spin along the orbital angular momentum produced in heavy-ion collisions. The global spin alignment of vector mesons ( $J^P = 1^-$ )  $\phi$  and  $K^{*0}$  may be sensitive to the vorticity in the medium and hadronization mechanisms. The second phase of RHIC Beam Energy Scan (BES-II) program provides higher statistics data sets for Au+Au collisions at  $\sqrt{s_{NN}} = 7.7-19.6$  GeV. From this data, we can make high precision measurements of  $\phi$  and  $K^{*0}$  global spin alignment, allowing for more differential studies not possible with the BES-I data. We can also compare global spin alignment between  $\phi$  and  $K^{*0}$ , where the lifetime of  $\phi$  is roughly ten times larger than that of  $K^{*0}$  and the latter is more sensitive to hadronic rescattering. We report high precision measurements for the global spin alignment of  $\phi$  at  $\sqrt{s_{NN}} = 19.6$  GeV from BES-II.

## 1 Introduction

In non-central heavy-ion collisions, a large orbital angular momentum (OAM) is generated. This OAM may preferentially align a particle's spin projection on the spin quantization axis through spin-orbit couplings, a phenomenon known as global spin alignment [1].

Preliminary results from the first phase of the RHIC Beam Energy Scan program (BES-I) showed a positive global spin alignment ( $\rho_{00} > 1/3$ ) for  $\phi$ -mesons and zero spin alignment ( $\rho_{00} \sim 1/3$ ) for  $K^{*0}$  mesons over the  $\sqrt{s_{NN}}$  of 11.5 to 200 GeV for Au+Au collisions [4]. The  $\sqrt{s_{NN}}$  dependence of the  $\phi$ -meson  $\rho_{00}$  can be accommodated by a theoretical model invoking a  $\phi$ -meson mean field, which is supported by the existence of this field [4,6,7]. In these proceedings, we present the  $\phi$ -meson global spin alignment from the BES-II Au+Au 19.6 GeV data set.

## 2 Analysis Details

As discussed, the global spin alignment of vector mesons is a measurement of the  $00^{th}$  component of the spin density matrix called  $\rho_{00}$ . This quantity can be extracted from a fit to the vector meson yield as a function of the daughter's angular distribution,

$$\frac{dN}{d(\cos \theta^*)} \propto (1 - \rho_{00}) + (3\rho_{00} - 1) \cos^2 \theta^*, \quad (1)$$

---

\*e-mail: gwilks3@uic.edu

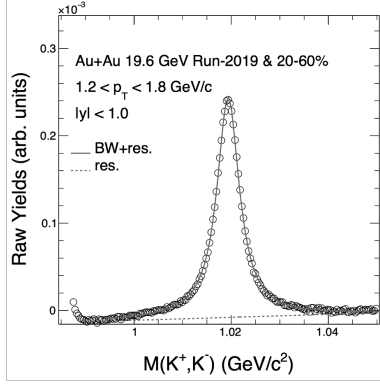


**Figure 1.** Invariant mass of  $K^+K^-$  pairs integrated over  $\cos\theta^*$  for 20-60% central Au+Au collisions at  $\sqrt{s_{NN}} = 19.6$  GeV. The solid line represents the combined fit of a Breit-Wigner and first order polynomial. The dashed lines is the first order polynomial, which is subtracted to extract the final yields.

32 where  $N$  is the number of  $\phi$ -mesons and  $\theta^*$  is the angle of the daughter  $K^+$  with respect to  
 33 the polarization axis in the parent's rest frame. The polarization axis is taken to be the orbital  
 34 angular momentum direction, which is estimated by the normal of the second order event  
 35 plane. The determination of the second order event plane in this analysis is achieved through  
 36 the use of the Time Projection Chamber (TPC) at STAR. To avoid self correlation and short  
 37 range non-flow contributions, we use the sub-event plane method for second order event  
 38 plane reconstruction [10]. Two sub-event windows were defined  $\eta_{east}(-1.0 < \eta < -0.05)$   
 39 and  $\eta_{west}(0.05 < \eta < 1.0)$  with an  $\eta$ -gap of 0.1. The second order sub-event plane resolution  
 40 achieved for mid-central collisions (20-60% centrality) was roughly 0.4. The acceptance  
 41 inefficiency of the detectors in STAR leads to a non-uniform event plane distribution and we  
 42 must therefore apply a recentering correction to the flow vector run-by-run for each centrality  
 43 and vertex  $z$  position range [11]. After the recentering correction a shift correction is applied  
 44 on an event-by-event basis to further correct for this non-uniformity [12].

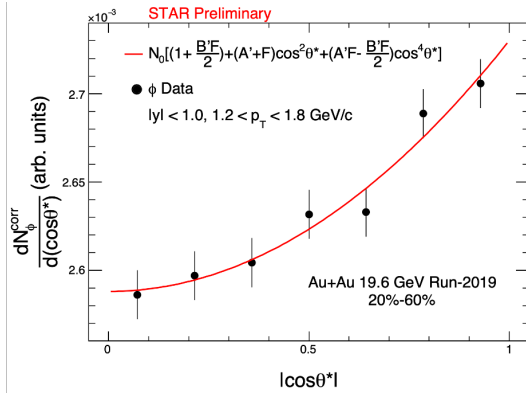


**Figure 2.** Efficiency corrected  $\phi$  meson yields as a function of  $\cos\theta^*$  for 20-60% central Au+Au collisions at  $\sqrt{s_{NN}} = 19.6$  GeV. The red line is the fit to the data used to extract  $\rho_{00}$ , given in detail by Eqs. (2-4). Only statistical uncertainties are shown.

45 In addition to the efficiency correction, we need to correct for the STAR detector's finite  
 46 acceptance in  $|\eta|$ , which can artificially contribute to the  $\rho_{00}$  signal. Also, since we are unable  
 47 to know the exact reaction plane, we must therefore correct for the effect of the event plane  
 48 resolution. The final fit function for the  $\cos\theta^*$  dependent yields is

$$\frac{dN^{\text{corr}}}{d(\cos\theta^*)} = N_0 \left[ \left(1 + \frac{B'F}{2}\right) + (A' + F) \cos^2\theta^* + \left(A'F - \frac{B'F}{2}\right) \cos^4\theta^* \right], \quad (2)$$

where

$$A' = \frac{A(1 + 3R)}{4 + A(1 - R)}, \quad B' = \frac{A(1 - R)}{4 + A(1 - R)}, \quad (3)$$

and

$$A = \frac{3\rho_{00} - 1}{1 - \rho_{00}}. \quad (4)$$

49 In the above equations,  $N^{corr}$  is the efficiency corrected yield,  $N_0$  is the normalization factor,  $R$   
 50 is the event plane resolution and  $F$  is the acceptance parameter found through STAR detector  
 51 simulations. Figure 2 shows an example of  $\phi$ -meson yield as a function of  $\cos \theta^*$ . Details of  
 52 the acceptance and resolution corrections can be found in [5].

### 53 3 Results and Discussion

54 In Figure 3, we show the  $\phi$ -meson  $\rho_{00}$  calculated for Au+Au collisions from BES-II at  $\sqrt{s_{NN}}$   
 55 = 19.6 GeV in four  $p_T$  bins at 20-60% centrality. The transverse momentum integrated global  
 56 spin alignment for  $\phi$ -meson at  $\sqrt{s_{NN}} = 19.6$  GeV from BES-II mid-central collisions was  
 57 measured to be  $\rho_{00} = 0.3622 \pm 0.0026$  (stat.)  $\pm 0.0049$  (sys.), which is larger than  $1/3$  with  
 58  $5.2\sigma$  significance. Further theoretical progress is needed to understand this  $p_T$  dependence  
 59 and is currently being investigated with a model invoking a  $\phi$ -meson mean field [6,7,8].

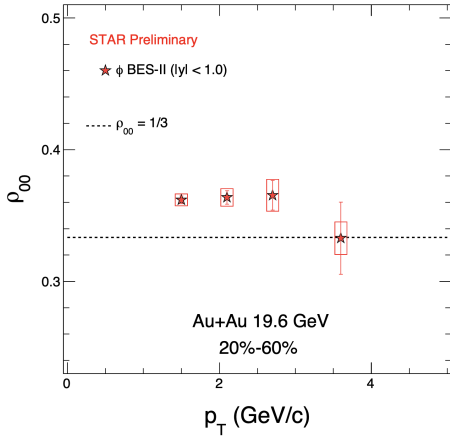


**Figure 3.**  $p_T$  dependent  $\rho_{00}$  for 20-60% centrality Au+Au collisions at  $\sqrt{s_{NN}} = 19.6$  GeV. The  $p_T$  dependence is currently being investigated using a  $\phi$ -meson mean field model [8]. The vertical lines are statistical uncertainties and boxes represent systematic uncertainties.

60 The analysis for  $\rho_{00}$  of  $K^{*0}$  is currently ongoing for the BES-II  $\sqrt{s_{NN}} = 19.6$  GeV data  
 61 set. In the BES-I results,  $K^{*0}$  was found to have no global spin alignment. This could be  
 62 due to  $K^{*0}$  having a roughly 10 times smaller lifetime than that of  $\phi$ , resulting in different  
 63 in medium interactions and a different late stage hadronic reaction [9]. Additionally, the  
 64 fluctuating vector meson fields for the  $d$  and  $\bar{s}$  quarks are expected to be weaker than  $s$  and  $\bar{s}$ ,  
 65 leading to a negligible contribution to  $\rho_{00}$  for  $K^{*0}$  [7].

### 66 4 Conclusion

67 We presented results for the  $\phi$ -meson  $\rho_{00}$  from the BES-II 19.6 GeV Au+Au data set. The  
 68 measured global spin alignment is significantly positive ( $\rho_{00} > 1/3$ ). Our precision is greatly  
 69 improved by the high-statistics BES-II data sets, which contains 478 million events for  $\sqrt{s_{NN}}$   
 70 = 19.6 GeV compared to 19 million in BES-I. This will allow us to perform differential  
 71 studies at these energies that were previously unachievable with the BES-I data sets, such as  
 72 centrality and rapidity dependent studies. These precise studies of vector meson  $\rho_{00}$  aim to  
 73 further theoretical progress towards understanding of this quantity and how it can be used to  
 74 probe other physical phenomena, such as spin polarization by a possible vector meson strong  
 75 force field.

## 76 **Acknowledgements**

77 The author is supported in part by The United States Department of Energy.

## 78 **References**

- 79 [1] Z. T. Liang and X. N. Wang, Phys. Lett. B **629**, 20–26 (2005).  
80 [2] F. E. Close, *An Introduction to Quarks and Partons* (Academic Press Inc. (London) 1979,  
81 481p, 1979).  
82 [3] K. Schilling et al., Nucl. Phys.B18, **332** (1970).  
83 [4] M.S. Abdallah et al. (STAR Collaboration), arXiv:2204.02302 (2022).  
84 [5] A. Tang et al., Phys. Rev. C **98**, 044907 (2018).  
85 [6] X.L. Sheng et al., Phys. Rev. D **101**, 096005 (2020).  
86 [7] X.L. Sheng et al., Phys. Rev. D **102**, 056013 (2020).  
87 [8] X.L. Sheng et al., arXiv:2205.15689 (2022).  
88 [9] I. Karpenko and F. Becattini, Eur. Phys. J. C **77**, 213 (2017).  
89 [10] A. M. Poskanzer and S. A. Voloshin, Phys. Rev. C **58**, 1671 (1998).  
90 [11] P. Danielewicz et al., Phys. Rev. C **38**, 120 (1988).  
91 [12] B. I. Abelev et al. (STAR Collaboration), Phys. Rev. C **81**, 044902 (2010).